

Comparison of Manual versus Automated Choroidal Thickness Measurements Using Swept-Source Optical Coherence Tomography

Khaled Abdelazeem, Dalia Mohamed El-Sebaity, Esraa Rifat Mokhtar¹, Ehab Wasfi, Momen Ahmad Mohammad Aly

Department of Ophthalmology, Faculty of Medicine, Assiut University, ¹Alforsan Eye Center, Assiut, Egypt

Abstract

Purpose: The purpose of this study was to compare the automated and manual choroidal thickness (CT) measures in normal eyes using swept-source optical coherence tomography (SS-OCT). **Patients and Methods:** This prospective study included 80 eyes from 40 normal volunteers. CT was measured manually and automatically in all eyes using Topcon deep-range imaging-1 SS-OCT. Automatically calculated measures, which are shown as a colored topographic map with nine subfields, defined by the Early Treatment Diabetic Retinopathy Study (ETDRS) style grid, compared to manual measures at the subfoveal area, at four points 1 mm around the fovea as well as at four points 3 mm around the fovea. **Results:** The mean subfoveal CT (SFCT) was $271.77 \pm 78.78 \mu\text{m}$ for the automatically measured ETDRS map and $282.81 \pm 83.74 \mu\text{m}$ for the manual SFCT measurements. The difference between manual and automated measurement was the smallest in SFCT at $11.03 \pm 35 \mu\text{m}$ and the greatest in the outer temporal area at $48.36 \pm 49.83 \mu\text{m}$. Manually measured CT was significantly higher ($P < 0.001$) in all nine areas compared to automated ETDRS map measurements. **Conclusions:** Manual measurement of CT is significantly higher than automated measurements. In addition, they cannot replace automated methods.

Keywords: Automated, choroidal thickness, manual, optical coherence tomography, swept source

INTRODUCTION

The choroid is a layer of connective tissue densely packed with blood vessels. As a major vascular layer of the eye, it supplies oxygen and nutrients to the retina and is vital to ocular health.^[1] Choroidal abnormalities such as vascular hyperpermeability, vascular changes, loss, and thinning play a significant role in the onset and progression of numerous posterior segment diseases. Choroid is involved in the pathogenesis of several diseases, such as age-related macular degeneration (AMD), myopic chorioretinopathy, central serous chorioretinopathy (CSCR), and polypoidal choroidal vasculopathy.^[2-6]

Choroidal thickness (CT) ranges from 170 to 220 μm and is essential for monitoring the development and progression of diseases that result in choroidal thinning. According to histologic studies,^[7] ultrasonography,^[8] magnetic resonance imaging,^[9] and Doppler laser have been used to study the choroid; however, the resolution was inadequate. In contrast, indocyanine green angiography provides clinical information but not CT.^[10]

Optical coherence tomography (OCT) is a noninvasive and noncontact imaging modality that enables two-dimensional, cross-sectional, and three-dimensional volumetric imaging of tissue architecture.^[11] It is currently considered one of the most essential tests in ophthalmic practice. It provides cross-sectional images with a high resolution of the retina, the retinal nerve fiber layer, and the optic nerve head.^[12] It is also helpful in imaging the anterior segment (AS) of the eye^[13] and for diagnosis and monitoring several AS diseases^[14-16] and evaluation of surgical procedures.^[17,18] Since 2006, spectral-domain OCT (SD-OCT) has been commercially available. Enhanced depth image OCT (EDI-OCT), which

Address for correspondence: Dr. Khaled Abdelazeem,
Department of Ophthalmology, Assiut University, Assiut 71515, Egypt.
E-mail: abdelazeem.kh@aun.edu.eg

This is an open access journal, and articles are distributed under the terms of the Creative Commons Attribution-NonCommercial-ShareAlike 4.0 License, which allows others to remix, tweak, and build upon the work non-commercially, as long as appropriate credit is given and the new creations are licensed under the identical terms.

For reprints contact: WKHLRPMedknow_reprints@wolterskluwer.com

How to cite this article: Abdelazeem K, El-Sebaity DM, Mokhtar ER, Wasfi E, Mohammad Aly MA. Comparison of manual versus automated choroidal thickness measurements using swept-source optical coherence tomography. *Egypt Retina J* 2022;9:26-30.

Submission: 01.05.2023

Acceptance: 06.05.2023

Web Publication: 30.05.2023

Access this article online

Quick Response Code:



Website:
www.egyptretinaj.com

DOI:
10.4103/erj.erj_3_23

allows quantitative thickness measurements of the choroid, was developed by Spaide *et al.*^[19] to permit choroidal imaging using SD-OCT devices.^[20-22] Another type of OCT instrument, swept-source OCT (SS-OCT), utilizes a tunable laser (SS) as a light source with a longer wavelength, allowing deeper tissue penetration than the SD-OCT. Numerous studies have confirmed the dependability and reproducibility of measurement CT using an SS-OCT device and assessed the normal CT in healthy individuals.^[23-26] The current study aimed to compare the CT measurements of normal eyes of healthy individuals with automated SS-OCT and manual measures.

PATIENTS AND METHODS

This prospective, cross-sectional study was approved by the Institutional Review Board of the Faculty of Medicine, Assiut University (approval number 17300719, dated January 23, 2022). All study procedures adhered to the tenets of the Declaration of Helsinki. All participants provided written informed consent to participate in the study following a discussion about the nature of the study and the risks/benefits of participation.

The study included 80 eyes of 40 normal Egyptian volunteers, between March 2022 and October 2022, at Alforsan Eye Centre, Asyut, Egypt. All the participants underwent full ocular examination, including measurement of uncorrected distant visual acuity, slit-lamp examination, autorefractometer KR-8900 (Topcon, Tokyo, Japan), axial length measurement using ocular biometry (intraocular lens Master; Carl Zeiss Meditec, Dublin, CA, USA), intraocular pressure measurement utilizing a Goldmann applanation tonometer, and dilated funduscopy after the application of 1% tropicamide eye drops.

Exclusion criteria included the presence of media opacity, chorioretinal or vitreoretinal diseases such as AMD, diabetic retinopathy, CSCR, epiretinal membrane, and macular dystrophy, history of intraocular surgery, and patients with glaucoma. Patients with systemic diseases or conditions that could affect retinal or CT, such as diabetes mellitus, Vogt–Koyanagi–Harada disease, or malignant hypertension, as well as pregnant females, were also excluded.

Swept-source optical coherence tomography system and scan protocols

A single expert retina specialist used a Topcon deep range imaging-1 SS-OCT for CT measurements (Topcon, Tokyo, Japan). Following pupillary dilatation with 1% tropicamide, a 12, 9-mm radial line scan protocol was executed. Each radial line was automatically scanned 32 times at the same location, followed by the creation of 12 average B-scan images with high resolution. Each scan was double-checked to confirm that it was centered on the fovea. Only scans of high quality were included.

The perpendicular distance between Bruch's membrane and the junction of the choroid and sclera was used to calculate CT. It was calculated automatically using the mapping

software incorporated into the device and displayed as a colorful topographic map with nine subfields defined by the Early Treatment Diabetic Retinopathy Study (ETDRS) style grid. It consists of three concentric rings centered in the fovea's center. The inner ring has a diameter of 1 mm, the middle ring has a diameter of 3 mm, and the outer ring has a diameter of 6 mm. The superior, inferior, nasal, and temporal quadrants were subdivided from the middle and outer rings. Afterward, an automatic topographic map of CT was created. The subfoveal CT (SFCT) at the inner ring, nasal inner macula, superior inner macula, temporal inner macula, inferior inner macula, nasal outer macula, superior outer macula, temporal outer macula, and inferior outer macula are the nine ETDRS subfields [Figure 1]. In the meantime, a three-dimensional macular technique was utilized to quantify the central macular thickness to rule out any retinal abnormalities.

The SFCT was measured manually from the outer border of the retinal pigment epithelium to the choroid-sclera junction. Simultaneously, CT was measured manually at eight points around the foveal center. For each quadrant around the fovea, CT was manually measured at a distance of 1 mm and 3 mm from the foveal center on the vertical [Figure 2] and horizontal line scans. The manual measures at 1 mm were compared to the corresponding areas of the inner ring for automated measures, while the manual measures at 3 mm were compared to the corresponding areas of the outer rings of the automated measures.

Statistical analysis

Data analysis was performed using the Statistical Package for the Social Sciences (IBM-SPSS Inc., Chicago, Illinois, USA) version 26.0 software. The Shapiro–Wilk test was used to determine the normality of all numerical variables before evaluation. Data were expressed using mean \pm standard deviation. The paired sample *t*-test was used to compare the means of manual and automated measurements. The level of significance was set at $P < 0.05$.

RESULTS

This prospective study included a total of 80 eyes from 40 normal Egyptian volunteers; 25 participants were female (62.5%), and 15 participants were male (37.5%). The age range was 18–46 years, with a mean of 27.6 ± 6.2 . The mean spherical equivalent (SE) of refractive error

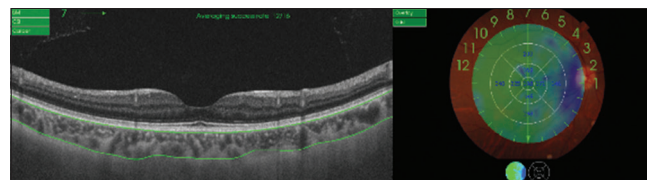


Figure 1: Automatically plotted colored topographic map of the nine subfields defined by the ETDRS map. ETDRS: Early Treatment Diabetic Retinopathy Study

SE was -3.59 ± 2.12 D (range: 0–10 D). The population characteristics are summarized in Table 1.

The deep structures of the posterior pole were visible using an SS-OCT system with a center wavelength of 1050 nm. Because of the higher penetration of the light source due to its longer operating wavelength and higher scan rate (100,000 Hz), no eye was excluded from the current study due to a low-quality image due to cataracts or eye movement during the scanning procedure.

Table 1: Characteristics of the studied participants

Variables	Mean±SD (range)
Age (years)	27.58±6.73 (18–46)
Gender, n (%)	
Male	15 (37.5)
Female	25 (62.5)
Manifest refraction sphere	-3.36 ± 2.34 (-10.00–1.00)
Cylinder	-0.92 ± 0.85 (-3.75–0.00)
Cylinder axis	92.62±64.06 (2–180)
Spherical equivalent of refractive error	-3.82 ± 2.33 (-10.00–0.50)
Central retinal thickness (µm)	240.63±20.29 (193–282)

SD: Standard deviation

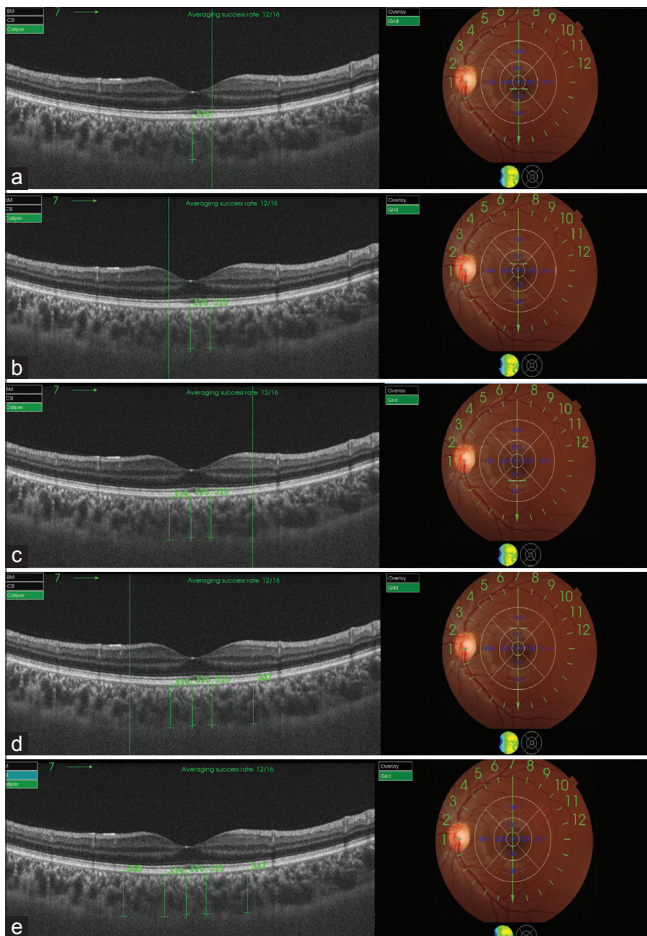


Figure 2: Manual measurement of the CT on the vertical meridian. (a) SFCT, (b) CT at 1 mm inferior to the fovea, (c) CT at 1 mm superior to the fovea, (d) CT at 3 mm inferior to the fovea, and (e) CT at 3 mm superior to the fovea. CT: Choroidal thickness, SFCT: Subfoveal choroidal thickness

The mean CT in the different subfields is listed in Table 2. The mean SFCT was 271.77 ± 78.78 (106–466) µm for the ETDRS map measurements and 282.81 ± 83.74 (103–492) µm for the manual SFCT measurements. A significant difference was found in CT between the two measurements, $P < 0.001$. The difference between the manual and automated measurements was the smallest in SFCT at 11.03 ± 35 µm and the greatest in the outer temporal area at 48.36 ± 49.83 µm. As shown in Table 2 and Figure 3, manually measured CT in nine areas was significantly higher ($P < 0.001$) than automated ETDRS map measurements.

The choroid is thicker in both manual and automated measures at the outer superior part, 326.06 ± 82.56 µm and 281.56 ± 65.37 µm, respectively. In contrast, the thinner part of the choroid was outer nasal in both manual and automated measures, 218.35 ± 79.25 µm and 200.94 ± 67.98 µm, respectively.

DISCUSSION

The choroid plays a crucial role in the pathophysiology of several retinal disorders. In several studies, choroidal abnormalities such as vascular hyperpermeability, vascular loss, and thinning have been found to be crucial in the onset and progression of retinal disorders.^[27] Recent SD-OCT advancements now provide two methods for determining CT: high-penetration OCT using a long-wavelength light source of 1060 nm^[28–30] and the EDI technique developed previously (SPECTRALIS OCT; Heidelberg Engineering).^[31] The SS-OCT uses a longer wavelength source (1050 nm), which facilitates accurate visualization of the corneal interface.^[32]

Multiple studies have characterized normal CT in healthy individuals. Ikuno *et al.*^[29] demonstrated an approximate SFCT of 354 µm in 43 Japanese volunteers with a mean age of 39.4 years using a 1060-µm-based light source. The superior, temporal, inferior, and nasal choroid values were 364, 337, 345, and 227 µm, respectively, at 3 mm to the fovea. These findings demonstrated a thicker choroid superiorly and thinner nasally, which is consistent with our results. Margolis and Spaide^[30] used an EDI approach to investigate SFCT in 30 normal participants (mean age: 50.4 years) and found that

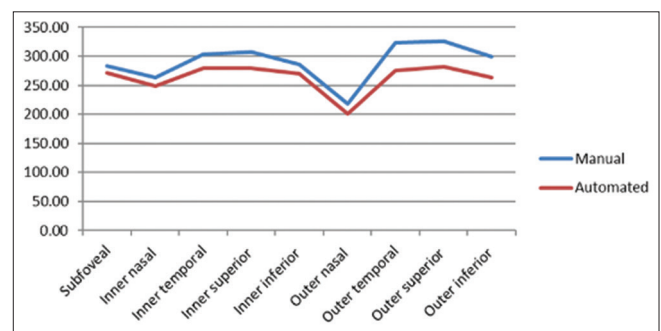


Figure 3: Manual versus automated CT measurements. CT: Choroidal thickness

Table 2: Manual and automated measurements

Variables	Mean ± SD (range)			P*
	Manual	Automated	Difference (manual-automated)	
Inner nasal	262.75±88.52 (106–502)	248.69±80.65 (89–460)	14.06±44.97 (–78.00–211.00)	<0.001
Outer nasal	218.35±79.25 (66–464)	200.94±67.98 (88–375)	17.41±40.45 (–78.00–201.00)	<0.001
Inner temporal	303.96±78.69 (148–491)	279.19±74.86 (137–472)	24.77±44.91 (–59.00–178.00)	<0.001
Outer temporal	323.63±77.96 (168–472)	275.26±66.90 (138–435)	48.36±49.83 (–85.00–163.00)	<0.001
Inner superior	307.81±73.38 (172–517)	279.16±71.95 (125–468)	28.65±47.66 (–135.00–148.00)	<0.001
Outer superior	326.06±82.56 (123–585)	281.56±65.37 (153–477)	44.50±61.97 (–87.00–230.00)	<0.001
Inner inferior	286.24±81.70 (116–466)	270.20±80.31 (103–436)	16.03±34.21 (–125.00–155.00)	<0.001
Outer inferior	299.34±87.83 (108–465)	263.35±71.90 (101–430)	35.98±36.95 (–127.00–120.00)	<0.001
Subfovea	282.81±83.74 (103–492)	271.77±78.78 (106–466)	11.03±35.42 (–77.00–124.00)	<0.001

*Paired sample *t*-test compares the mean between manual and automated measurement. SD: Standard deviation

the choroid was the thickest beneath the fovea (287 μm) and then rapidly dropped nasally, averaging only 145 μm at 3 mm nasal to the fovea.

In research by Spaide *et al.*,^[19] the mean SFCT in 17 participants (mean age 33.4 years) utilizing an EDI system was 318 μm in the right eyes and 335 μm in the left eyes. In 210 healthy patients with a mean age of 49.73 years, CT was 261.93 μm subfoveal, 224.21 μm, 3 mm temporally, and 142.92 μm, 3 mm nasally. These results are relatively comparable to those published by Margolis and Spaide^[30] using an EDI system.

Although automated software for the measurement of macular or CT is a fast, accurate, and reliable method, it may result in incorrect measurements in nonhealthy eyes.^[33,34] Therefore, the manual measurement could be better in some cases.^[35] Lee *et al.*^[36] reported comparable results of repeatability of manual and automated CT measurements.

In the current study, we found a significant difference between manual and automated measures of CT in all ETDRS areas. The difference was less in the SFCT, 11.03 ± 35 μm. The thickness was higher when measured manually. This result may be because automated software measures thickness in an area; whereas our method measures thickness at a single point within this area. Comparing CT in healthy eyes and eyes with diseases causing choroidal thinning and thickening requires further research.

Financial support and sponsorship

Nil.

Conflicts of interest

There are no conflicts of interest.

REFERENCES

- Nickla DL, Wallman J. The multifunctional choroid. *Prog Retin Eye Res* 2010;29:144-68.
- Gupta B, Mohamed MD. Photodynamic therapy for variant central serous chorioretinopathy: Efficacy and side effects. *Ophthalmologica* 2011;225:207-10.
- Grossniklaus HE, Green WR. Choroidal neovascularization. *Am J Ophthalmol* 2004;137:496-503.
- Gomi F, Tano Y. Polypoidal choroidal vasculopathy and treatments. *Curr Opin Ophthalmol* 2008;19:208-12.
- Rajendram R, Evans M, Rao NA. Vogt-Koyanagi-Harada disease. *Int Ophthalmol Clin* 2005;45:115-34.
- Fitzgerald ME, Wildsoet CF, Reiner A. Temporal relationship of choroidal blood flow and thickness changes during recovery from form deprivation myopia in chicks. *Exp Eye Res* 2002;74:561-70.
- Guyer D, Schachat A, Green W. The choroid: Structural considerations. *Retina* 2006;1:1831-64.
- Coleman DJ, Lizzi FL. *In vivo* choroidal thickness measurement. *Am J Ophthalmol* 1979;88:369-75.
- Cheng H, Nair G, Walker TA, Kim MK, Pardue MT, Thulé PM, *et al.* Structural and functional MRI reveals multiple retinal layers. *Proc Natl Acad Sci U S A* 2006;103:17525-30.
- Stanga PE, Lim JI, Hamilton P. Indocyanine green angiography in chorioretinal diseases: Indications and interpretation: An evidence-based update. *Ophthalmology* 2003;110:15-21.
- Huang D, Swanson EA, Lin CP, Schuman JS, Stinson WG, Chang W, *et al.* Optical coherence tomography. *Science* 1991;254:1178.
- Sull AC, Vuong LN, Price LL, Srinivasan VJ, Gorczyńska I, Fujimoto JG, *et al.* Comparison of spectral/Fourier domain optical coherence tomography instruments for assessment of normal macular thickness. *Retina* 2010;30:235-45.
- Ramos JL, Li Y, Huang D. Clinical and research applications of anterior segment optical coherence tomography – A review. *Clin Exp Ophthalmol* 2009;37:81-9.
- Abdelazeem K, Sharaf M, Saleh MG, Fathalla AM, Soliman W. Relevance of swept-source anterior segment optical coherence tomography for corneal imaging in patients with flap-related complications after LASIK. *Cornea* 2019;38:93-7.
- Soliman W, Nassr MA, Abdelazeem K, Al-Hussaini AK. Appearance of herpes simplex keratitis on anterior segment optical coherence tomography. *Int Ophthalmol* 2019;39:2923-8.
- Soliman W, Mohamed TA. Spectral domain anterior segment optical coherence tomography assessment of pterygium and pinguecula. *Acta Ophthalmol* 2012;90:461-5.
- Doors M, Berendschot TT, de Brabander J, Webers CA, Nuijts RM. Value of optical coherence tomography for anterior segment surgery. *J Cataract Refract Surg* 2010;36:1213-29.
- Abdelazeem K, Nassr MA, Abdelmotaal H, Wasfi E, El-Sebaity DM. Flap sliding technique for managing flap striae following laser *in situ* keratomileusis. *J Ophthalmol* 2020;2020:5614327.
- Spaide RF, Koizumi H, Pozzoni MC. Enhanced depth imaging spectral-domain optical coherence tomography. *Am J Ophthalmol* 2008;146:496-500.
- Huber R, Adler DC, Srinivasan VJ, Fujimoto JG. Fourier domain mode locking at 1050 nm for ultra-high-speed optical coherence tomography of the human retina at 236,000 axial scans per second. *Opt Lett* 2007;32:2049-51.
- Lim H, de Boer JF, Park BH, Lee EC, Yelin R, Yun SH. Optical frequency domain imaging with a rapidly swept laser in the 815-870 nm

- range. *Opt Express* 2006;14:5937-44.
22. Unterhuber A, Povazay B, Hermann B, Sattmann H, Chavez-Pirson A, Drexler W. *In vivo* retinal optical coherence tomography at 1040 nm – Enhanced penetration into the choroid. *Opt Express* 2005;13:3252-8.
 23. Copete S, Flores-Moreno I, Montero JA, Duker JS, Ruiz-Moreno JM. Direct comparison of spectral-domain and swept-source OCT in the measurement of choroidal thickness in normal eyes. *Br J Ophthalmol* 2014;98:334-8.
 24. Ruiz-Moreno JM, Flores-Moreno I, Lugo F, Ruiz-Medrano J, Montero JA, Akiba M. Macular choroidal thickness in normal pediatric population measured by swept-source optical coherence tomography. *Invest Ophthalmol Vis Sci* 2013;54:353-9.
 25. Mokhtar E, Abdelazeem K, Abdalla A, Fahmy H. Factors affecting choroidal thickness in normal myopic eyes in Egyptians using swept-source optical coherence tomography. *Egypt Retin J* 2018;5:35-40.
 26. Moussa M, Sabry D, Soliman W. Macular choroidal thickness in normal Egyptians measured by swept source optical coherence tomography. *BMC Ophthalmol* 2016;16:138.
 27. Ding X, Li J, Zeng J, Ma W, Liu R, Li T, *et al.* Choroidal thickness in healthy Chinese subjects. *Invest Ophthalmol Vis Sci* 2011;52:9555-60.
 28. Regatieri CV, Branchini L, Fujimoto JG, Duker JS. Choroidal imaging using spectral-domain optical coherence tomography. *Retina* 2012;32:865-76.
 29. Ikuno Y, Kawaguchi K, Nouchi T, Yasuno Y. Choroidal thickness in healthy Japanese subjects. *Invest Ophthalmol Vis Sci* 2010;51:2173-6.
 30. Margolis R, Spaide RF. A pilot study of enhanced depth imaging optical coherence tomography of the choroid in normal eyes. *Am J Ophthalmol* 2009;147:811-5.
 31. Narendran S, Manayath G, Venkatapathy N. Comparison of choroidal thickness using swept-source and spectral-domain optical coherence tomography in normal Indian eyes. *Oman J Ophthalmol* 2018;11:38-41.
 32. Chung SE, Kang SW, Lee JH, Kim YT. Choroidal thickness in polypoidal choroidal vasculopathy and exudative age-related macular degeneration. *Ophthalmology* 2011;118:840-5.
 33. Twa MD, Schulle KL, Chiu SJ, Farsiu S, Berntsen DA. Validation of macular choroidal thickness measurements from automated SD-OCT image segmentation. *Optom Vis Sci* 2016;93:1387-98.
 34. Yang CS, Cheng CY, Lee FL, Hsu WM, Liu JH. Quantitative assessment of retinal thickness in diabetic patients with and without clinically significant macular edema using optical coherence tomography. *Acta Ophthalmol Scand* 2001;79:266-70.
 35. Taban M, Sharma S, Williams DR, Waheed N, Kaiser PK. Comparing retinal thickness measurements using automated fast macular thickness map versus six-radial line scans with manual measurements. *Ophthalmology* 2009;116:964-70.
 36. Lee S, Fallah N, Forooghian F, Ko A, Pakzad-Vaezi K, Merkur AB, *et al.* Comparative analysis of repeatability of manual and automated choroidal thickness measurements in nonneovascular age-related macular degeneration. *Invest Ophthalmol Vis Sci* 2013;54:2864-71.